Dendrochronologia 47 (2018) 1–9

Contents lists available at ScienceDirect

Dendrochronologia

journal homepage: www.elsevier.com/locate/dendro

Growth response of *Abies georgei* to climate increases with elevation in the central Hengduan Mountains, southwestern China

Shankar Panthi[a,b], Achim Bräuning[c], Zhe-Kun Zhou[a], Ze-Xin Fan[a,*]

[a] Key Laboratory of Tropical Forest Ecology, Xishuangbanna Tropical Botanical Garden, Chinese Academy of Sciences, Menglun, Mengla, Yunnan 666303, China
[b] University of Chinese Academy of Sciences, Beijing 100049, China
[c] Institute of Geography, University of Erlangen-Nürnberg, Erlangen, Germany

ARTICLE INFO

Keywords:
Yunnan fir (*Abies georgei*)
Climate variability
Elevational trend
Hengduan Mountains
High-elevation forests
Tree rings

ABSTRACT

Climatic harshness is expected to increase at higher elevations; however, elevational trends of tree radial growth response of high-elevation forests to climate change need to be investigated at different locations because of existing local variability in site-specific climatic conditions. We developed tree-ring width chronologies of Yunnan fir (*Abies georgei*) along elevation gradients at two sites in the central Hengduan Mountains (HM). High-elevation forests of *A. georgei* showed growth synchronicity and common growth signals along elevation gradients, indicating a common climatic forcing, although tree radial growth rates decreased with increasing elevation. Radial growth of Yunnan fir showed positive correlations with summer temperatures and February precipitation and moisture availability, but were negatively correlated with spring temperatures. The strongest positive relationship indicated summer (July) mean and minimum temperatures are the most important growth determining climatic factors for tree radial growth in the cold environment of HM, and this relationship revealed a clear elevational trend with stronger correlations at higher altitudes. In contrast, tree radial growth was negatively correlated with June precipitation and moisture availability. The whole study period 1954–2015 was split in two sub-periods of equal length. Comparing the early sub-period (1954–1984) to the later sub-period (1985–2015), tree growth response to the summer temperatures strongly increased, while it became weaker to June precipitation and moisture availability. High-elevation Yunnan fir forests in the HM currently benefit from elevated growing season temperatures under humid summer conditions. However, increasing temperatures may induce drought stress on tree radial growth if the observed decreasing trend in humidity and precipitation continues.

1. Introduction

High-mountain regions are experiencing higher rates of temperature change than surrounding lowlands (Mountain Research Initiative EDW Working Group, 2015). Higher rates of climate change in Mountain ecosystems have a critical impact on the vegetation phenology, growth, productivity and dynamics of high-elevation forests (Liang et al., 2014, 2016; Yang et al., 2017). In high mountain environments, radial tree growth at high elevations is mostly temperature-limited (Bräuning, 2001; Fan et al., 2008a; Körner, 2012), whereas tree growth at lower elevations is more sensitive to precipitation variations (Schweingruber, 1996; Körner, 2012). Moreover, climatic harshness increases along elevation gradients and eventually radial tree growth may respond in different ways or to a different extent at different elevations (Lyu et al., 2016). Thus, a better understanding of growth responses to climate change along elevation gradients could help to predict changes in growth dynamics and potential ecosystem vulnerability of high-elevation forests under climate change (Fan et al., 2009a).

The central Hengduan Mountains (HM) is a transition zone of subtropical and temperate climate (Böhner, 2006) and characterized as a climatologically sensitive region (Fan et al., 2011; Fan and Thomas, 2013). The region is biogeographically complex and has been recognized as one of biodiversity hotspots with a high number of endemism and endangered plant species (Myers et al., 2000; Frenzel et al., 2003; Kier et al., 2005; Xing and Ree, 2017). Due to complex topography and wide variety of microclimates, the HM harbor diverse vegetation types. Yunnan fir (*Abies georgei*) along with other high-elevation conifers is an important component of subalpine forest ecoregions in the central HM (Zhang et al., 2008). Tree growth of high-elevation forests in the HM could response differently along environmental gradients to local climatic variability and long-term climatic trends. Therefore, the study of elevational trends of climate-growth responses

* Corresponding author.
E-mail address: fanzexin@xtbg.org.cn (Z.-X. Fan).

https://doi.org/10.1016/j.dendro.2017.11.001
Received 30 May 2017; Received in revised form 26 October 2017; Accepted 17 November 2017
Available online 21 November 2017
1125-7865/ © 2017 Elsevier GmbH. All rights reserved.

of high-elevation forests is a relevant issue in the HM.

The HM have experienced a prominent warming trend during the past decades (0.3 °C/decade, Fan et al., 2011). In current scenarios of global climate change, radial tree growth in temperature-limited high-elevation forest ecosystems of the HM may benefit from rising temperatures (Fan et al., 2008a, 2009a) by an earlier start of cambial activity (Begum et al., 2013). This will result in both a higher rate of xylem cell production and a longer duration of cambial activity (Rossi et al., 2014), which in turn should trigger increased radial growth. Existing studies on radial tree growth responses to climate in the HM region indicate that radial growth at lower elevations is limited by spring moisture availability (Fan et al., 2009a) in the pre-summer monsoon season, a situation which could be aggravated with increasing temperatures. Other studies on climate-growth responses and growth dynamics were conducted on high-elevation forests in the HM (Fan et al., 2009a) and in nearby regions of Tibetan plateau (TP) (Yang et al., 2017) including south (Liu et al., 2013), south-eastern (Li et al., 2013; Liu et al., 2013; Lyu et al., 2016), and north-eastern Tibet (Liang et al., 2016), and western Sichuan (Li et al., 2012a). Most of the climate-growth response studies have been confined to the alpine treeline/timberline ecotone (ATE) of high mountains, while others were conducted for climate reconstruction purposes in the HM (Fan et al., 2008a,b, 2009b; Li et al., 2012b). A few studies were conducted on elevational trends of climate-growth responses in nearby regions (Liang et al., 2010, 2016; Li et al., 2012a; Liu et al., 2013; Lyu et al., 2016, 2017; Wang et al., 2017), however studies on elevational trends of climate-growth responses of high-elevation forests in the HM are rather scant (Fan et al., 2009a).

In this study, we aimed at exploring the dominant climatic factors that determine radial tree growth of high-elevation forests of *Abies georgei* along elevation gradients in the Hengduan Mountains, and to determine elevational trends in growth rates. According to the hypothesis that plant growth in cold high-elevation environments is controlled by temperature-limited physiological processes (Körner, 2015), we expected that tree radial growth at temperature-limited high mountain forests and at timberlines benefit from increasing temperatures (Körner, 2012). However, radial tree growth at lower elevations encounters more serious moisture limitation due to elevated temperature (Wang et al., 2017).

2. Materials and methods

2.1. Study area and climate

The study was conducted in the high-elevation forest ecosystems of the central Hengduan Mountains (HM), south-western China. The study sites are located in the Baima Snow Mountain (BSM) and Shika Snow Mountain (SSM) (Fig. 1). The HM forms the transitional zone between the south-eastern Tibetan Plateau, the north-western edge of the Yunnan Plateau and southern Sichuan, and extend from north-west to south-east. The region is characterized by complex topography due to deeply incised north–south oriented parallel gorges of the four major Asian rivers Mekong, Yangtze, Salween and Irrawaddy (Fan et al., 2009a,b). The topographical complexity creates distinct altitudinal belts and vegetation types with a high degree of plant endemism.

The climate of the HM is influenced by both maritime and continental air masses due to Asian monsoon climate with a seasonal change of wind systems with a warm and wet summer and relatively cold and dry winter (Böhner, 2006; Fan et al., 2009a). The continental air masses with occasional surges of dry continental polar air from northwesterly directions cause the cold and dry winters with snowfall and frost from November to April (Böhner, 2006). During summer (June to September), the heated Tibetan Plateau acts as a 'driving force' for the passage of monsoonal air masses originating from the Indian Ocean in the southwesterly direction causing heavy rainfall in the central Hengduan Mountains. The total annual precipitation of Deqin nearby BSM (Fig. 1) is 643 mm, 59% of which falls in summer, whereas spring (March–May) precipitation accounts for 25% of annual precipitation (Fig. 2a, Table 1). The average annual maximum, mean, and minimum temperatures at Deqin station are 11.70 °C, 5.51 °C, and 1.71 °C respectively, with a mean temperature of 12.64 °C in July and −2.28 °C in January (Fig. 2b, Table 1). While, at Shangri-la station situated near to SSM (Fig. 1), the total annual precipitation is 625 mm, 73.5% of which falls in summer, whereas spring precipitation accounts only for 14%. The average annual maximum, mean, and minimum temperatures at Shangri-la are 13.55 °C, 6.01 °C, and 0.19 °C respectively, with a mean temperature of 13.67 °C in July and −2.87 °C in January (Table 1). The low-level cloud cover (LCC) increases with the onset of the summer monsoon in June (or late May), which results in increasing precipitation and relative humidity (RH). As a consequence, abrupt decrease in total sunshine duration (SSD) occurs in our study sites in HM (Fig. 2), since LCC has strong inverse relationship with total SSD (Xia, 2010). The total annual and October to May SSD is higher at Shangri-la station, while the total SSD during summer is considerably lower at Deqin (Fig. 2c, d, Table 1). Similarly, the total amount of winter and spring precipitation at Shangri-la is considerably lower than at Deqin (Fig. 2a, b, Table 1).

Significant warming trends have been observed in annual temperatures over the past six decades at both Deqin and Shangri-la stations (Fig. 3). The annual mean temperatures have been increasing by 0.33 °C and 0.37 °C per decade at Deqin and Shangri-la stations, respectively (Fig. 3b). Compared to mean temperatures, warming trend was much higher for maximum temperatures (0.44 °C/decade) at Deqin (Fig. 3a), while the highest warming trend has been observed for minimum temperatures (0.63 °C/decade) at Shangri-la (Fig. 3c). No significant changes over time have been observed for annual precipitation in both stations (Fig. 3e). Annual mean relative humidity (RH) has decreased significantly at both Deqin and Shangri-la station (Fig. 3e). The decreasing trend of mean RH is more pronounced in Shangri-la and significant in all the months throughout the year, while in Deqin, decreasing trends of RH are significant only in February, and May-August (Table S1).

2.2. Tree-ring data

Abies georgei Orr var. *georgei* (Yunnan fir) is native in the central Hengduan Mountains including SW Sichuan, NW Yunnan, and SE Xizang provinces (Wu and Raven, 1999; Zhang et al., 2008) and endemic to China (Zhang et al., 2008). The species is cold tolerant and adapted to humid cold climate on north-facing slopes of high mountains. It is the dominant species in high-elevation montane forests and typically forms pure stands at the upper alpine timberline ecotone (ATE). Below ATE and at lower elevations, it forms either pure or mixed forest stands. Frequent fogs and convective clouds maintain humid conditions for the fir forests during the summer monsoon season. In the central HM, Yunnan fir has a rather narrow altitudinal distribution from 3700 m up to ATE, which is located at 4400 m in Baima Snow Mountain (BSM) and at 4200 m in Shika Snow Mountain (SSM).

Tree-ring increment cores of Yunnan fir were sampled along elevation gradients from the high-elevation upper montane forest stands at BSM and SSM in the HM in three elevational bands at 3900 m, 4200 m and 4400 m (ATE) in BSM and two elevational bands at 3900 m and 4200 m (ATE) in SSM (Table 2). In each elevational band, mature and healthy living trees were selected for sampling. Two increment cores per tree were collected using an increment borer. About 60 or more trees were sampled in each elevational band (Table 2).

We followed standard dendrochronological techniques for sample preparation and chronology development (Stokes and Smiley, 1996; Cook and Briffa, 1990). Wood surfaces of increment cores were smoothed to make ring boundaries clearly visible by using sanding papers with consecutively finer grit. Ring-width measurements were performed with a resolution of 0.001 mm under a stereomicroscope,

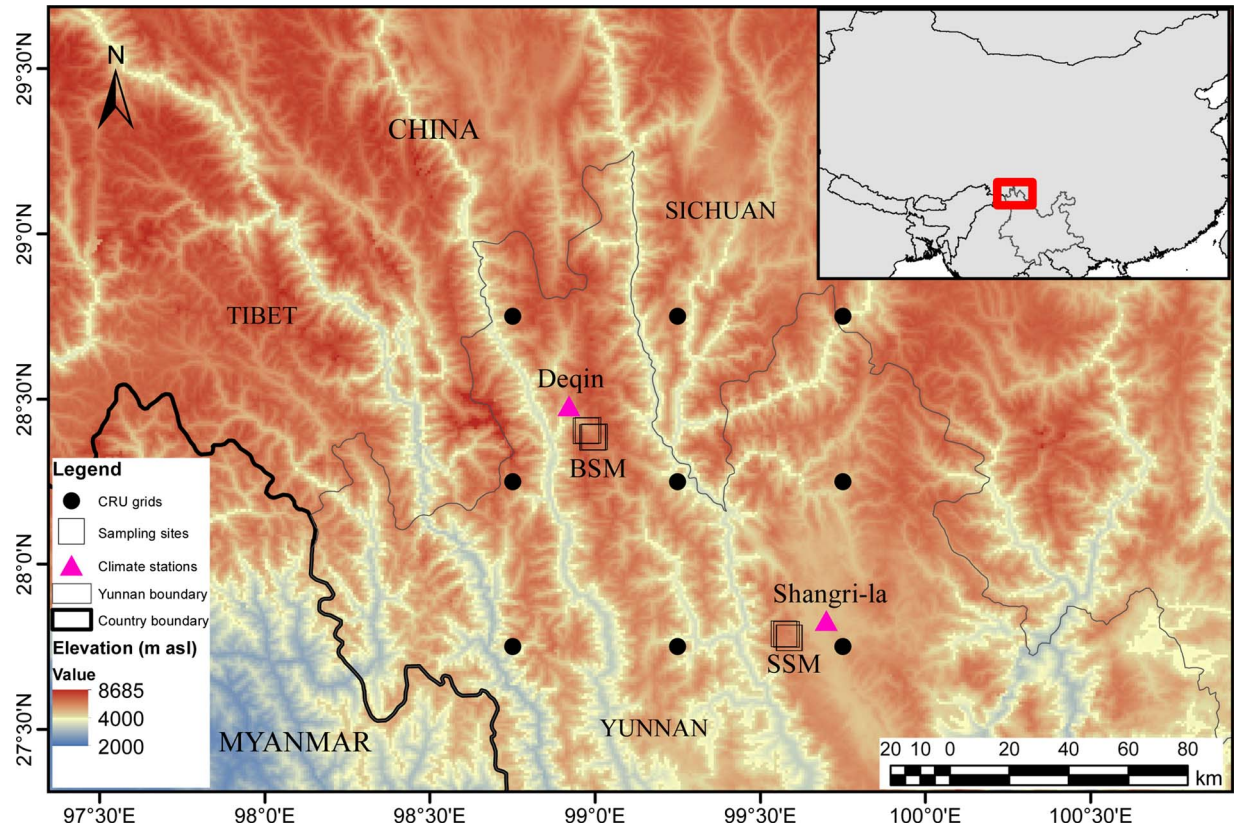

Fig. 1. Map of the study area showing sampling sites of Yunnan fir, climate stations and climatic research unit (CRU) grid points in the central Hengduan Mountains.

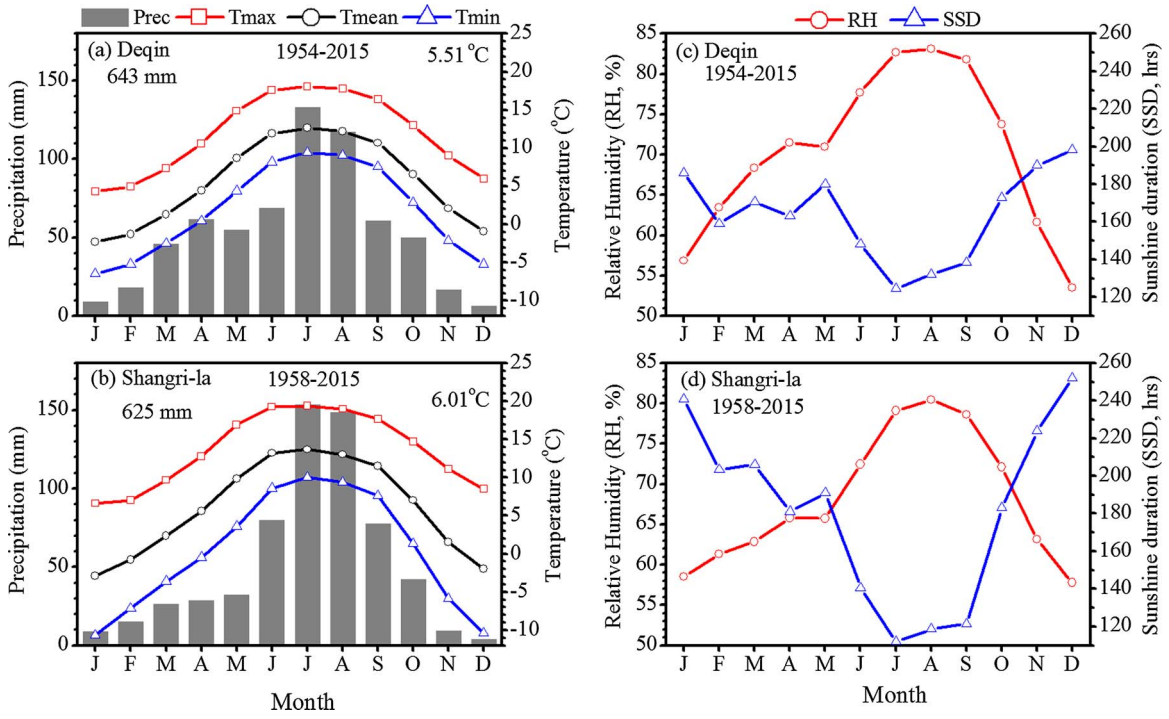

Fig. 2. Climate diagrams of study area showing monthly temperatures and precipitation (left panel), and monthly mean relative humidity and total sunshine duration (right panel) at Deqin station during 1954–2015 (a and c), and Shangri-la station during 1958–2015 (b and d) in the central Hengduan Mountains.

which was linked to a LINTAB digital positioning table (LINTAB™ 6, Rinntech, Germany). The tree-ring measurements were cross-dated to the calendar year of their formation by visual growth pattern matching and statistical tests (sign-test and *t*-test), using the software package TSAP-Win (Stokes and Smiley, 1996; Rinn, 2003). Finally, a total of 650/332 cores/trees (438/225 cores/trees in the BSM and 212/107 cores/tress in the SSM) of Yunnan fir were cross-dated (Table 2).

We standardized the raw ring-width measurements into dimensionless time series of ring-width indices (RWI) to remove biological growth trends related to tree-age and effects of stand dynamics on

Table 1
An overview on climate at the study sites in the Hengduan Mountains. CRU, Climatic research unit; NMIC, National Meteorological Information Center, China; BSM, Baima Snow Mountain; SSM, Shika Snow Mountain. Numbers in parentheses indicate percent of annual mean precipitation.

Station	Deqin	Shangrila	Regional CRU data
Data Source	NMIC	NMIC	CRU TS3.24, SPEI3.23
Span	1954–2015	1958–2015	1950–2015
Elevation (m asl)	3320	3277	–
Latitude (°N)/Longitude (°E)	28.48/98.92	27.83/98.76	27.75–28.75/ 98.75–99.75
Mean Temperature (°C)			
Annual	6.01	5.51	5.70
March–May	5.92	4.82	5.22
July	12.64	13.67	12.41
January	−2.28	−2.87	−2.03
Total Precipitation (mm)			
Annual	642.7	624.7	824.9
June–September	380.0 (59.0%)	459.0 (73.5%)	583.5 (70.7%)
March–May	162.5 (25.3%)	86.4 (13.8%)	143.0 (17.3%)
Sunshine duration (hours)			
Annual	1963.59	2173.91	–
March–May	513.84	577.98	–
June–September	543.44	492.62	–

ring-width variations, while preserving growth variations that are probably related to climate variability (Fritts, 1976; Cook, 1985). Data-adaptive power transformation was used to stabilize the variance of each series based on the individual mean and standard deviation (Cook and Peters, 1997). We applied a 'double-detrending' standardization: firstly, tree-ring series were detrended by a negative exponential or zero slope linear regression function as residual or differences, and then the resulted sequences were detrended with a cubic smoothing spline with a 50% frequency-response cut-off equal to 67% the series length (Cook and Peters, 1997). A mean function ring-width index (RWI) series was developed by computing a biweight robust mean to describe overall tree growth at a site, as well as to reduce the influence of outliers in tree-ring indices (Briffa and Jones, 1990; Cook and Briffa, 1990). We used the Briffa Rbar-weighted method to stabilize variance in order to reduce the potential influence of decreasing sample depths (Osborn et al., 1997). Residual chronologies were produced to remove any autocorrelation effect and the influence of previous year's growth from the tree-ring signals for each elevation band.

Average radial growth rate (AGR), standard deviation (SD), mean sensitivity (MS), and first-order autocorrelation (AC1) were calculated for raw ring-width series. The SD estimates the variability from the mean of ring-width series, the MS determines year-to-year variability on tree growth and AC1 assesses previous year influence on the current year growth (Fritts, 1976). The signal-to-noise ratio (SNR) was calculated for the common period analysis. SNR indicates the climatic strength retained in chronology where the noise is partially cancelled (Wigley et al., 1984). The mean inter-series correlation (Rbar) and expressed population signal (EPS) were calculated with a 30-year moving windows and 15-year overlaps. Rbar is the strength of the common signal between individual tree-ring series of a site and confirms the growth synchrony among the individual tree-ring series, while an EPS is a function of Rbar and the sample size and estimates the variance fraction of an infinite, hypothetical population expressed by the chronology. An EPS value 0.85 is considered as a suitable arbitrary threshold with shared population variance of 85% to indicate the reliable quality of a chronology (Wigley et al., 1984; Briffa and Jones, 1990). We performed Pearson correlation analysis and principal component analysis (PCA) to identify the growth similarity and the extent of growth coherency among residual chronologies for their common period along elevation gradients of both study sites. PCA extracts the maximum common variance in its first principal component (PC1) from the total variance of data and thus indicates the common growth signal.

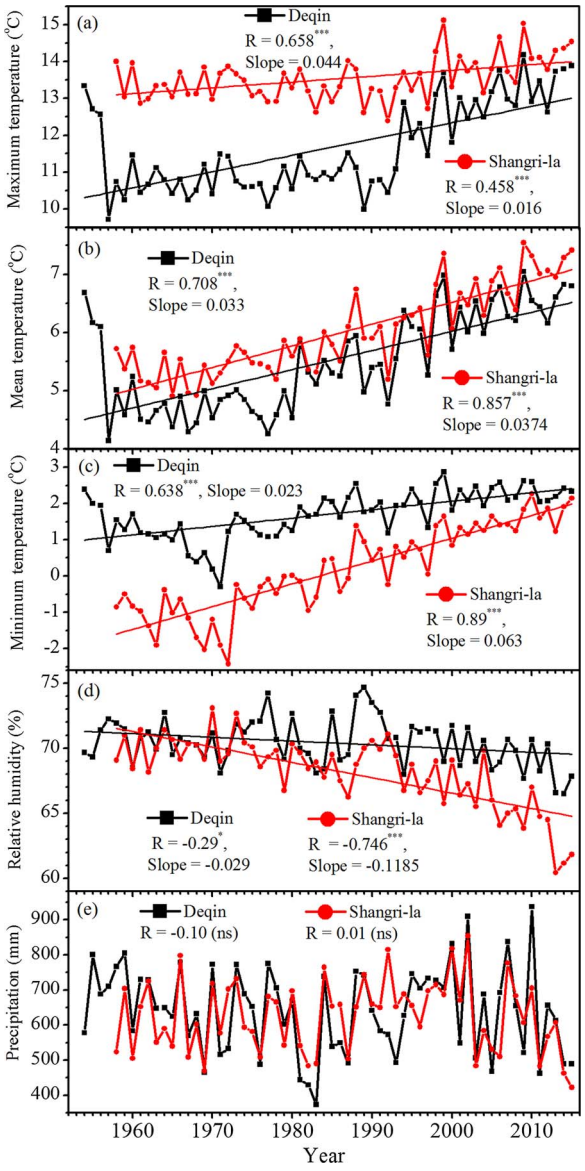

Fig. 3. Annual climate trends at Deqin (1954–2015, black line) and Shangri-la (1958–2015, red line) climate stations in the central Hengduan Mountains: (a) maximum temperature, (b) mean temperature, (c) minimum temperature, (d) mean relative Humidity (RH), (e) total precipitation. R represents correlation coefficient over the time. Significance: * $p < 0.05$, ** $p < 0.01$, *** $p < 0.001$. (For interpretation of the references to color in this figure legend, the reader is referred to the web version of this article.)

2.3. Tree growth response to climate

The monthly instrumental records (including precipitation, temperature and RH) for Deqin and Shangri-la stations were obtained from the National Meteorological Information Centre (NMIC), China. In addition, we used Standardized Precipitation-Evaporation Index (SPEI, Vicente-Serrano et al., 2010) datasets to test the influence of regional moisture conditions on tree growth variability. The SPEI datasets were obtained from the CRU grids (CRUTS3.23, http://sac.csic.es/spei) at half-degree spatial resolution. SPEI is a multi-scalar drought index, which integrates precipitation and potential evapotranspiration, as well as increased temperature induced water demand (Vicente-Serrano et al., 2010).

Table 2
Statistics of tree-ring width residual chronologies along elevation gradients. BSM, Baima Snow Mountain; SSM, Shika Snow Mountain; MSL/LSL, mean/longest segment length; AGR, average annual radial growth rate (mm); SD, standard deviation; MS, mean sensitivity; AC1, first-order autocorrelation; Rbar, mean inter-series correlation; SNR, signal-to-noise ratio; EPS, Expressed population signal. The SNR and EPS were calculated for the common period 1900–2010. AGR, SD, MS and AC1 were calculated for raw ring-width series. Site codes represent the elevation bands.

Site	Site code	Cores/Trees	Span	MSL/LSL	AGR	SD	MS	AC1	Rbar	SNR	EPS
BSM	B2_4400	182/92	1640–2015	155/376	0.487	0.214	0.156	0.865	0.514	7.11	0.989
	B2_4200	140/72	1636–2015	130/380	0.738	0.344	0.173	0.867	0.510	50.48	0.981
	B2_3900	116/61	1656–2015	122/360	0.998	0.452	0.164	0.876	0.435	31.18	0.969
SSM	S2_4200	105/52	1734–2015	110/282	1.230	0.372	0.137	0.810	0.464	9.92	0.908
	S2_3900	107/55	1640–2015	118/376	1.258	0.530	0.165	0.842	0.398	7.81	0.887

Climate-growth relationships were determined by using Pearson's correlation analyses. Correlations were computed between the tree-ring data (residual chronologies) of BSM and SSM, and monthly series of climate data (including temperature, precipitation, RH, and regional SPEI) for a 15-month window from previous year August to current year October. The BSM data were analyzed with instrumental records of Deqin station and SSM data with that of Shangri-la station. To test the growth sensitivity to the temporal change of climate, climate-growth relationships were analyzed over two different sub-periods and entire period of climate data: 1954–1984, 1985–2015 and 1954–2015 for BSM, and 1958–1984, 1985–2015 and 1958–2015 for SSM. Moreover, the SPEI datasets from nine CRU grid points over the whole region were averaged to get the regional moisture data, and the regional SPEI dataset was used to compute correlations with tree-ring data of BSM and SSM to observe influence of regional moisture conditions. We computed correlation with first-difference of climate data to overcome the autocorrelation effect due to significant trends in the original climate series (Fig. 3).

3. Results

Five new chronologies were developed along elevation gradients from the two sites (three for BSM and two for SSM) in the HM, spanning 360–380 years in the BSM site, and 282–376 years in the SSM site (Fig. 4, Table 2). All ring-width residual chronologies showed strong and consistent common signals along the elevational gradients in both sites (Fig. 4) over their common period of 1850–2015 (Table 3), with an average across-site correlation of 0.582 ($p < 0.001$). Correlations were higher between neighboring elevation bands than between distant elevation bands of the same site. Principal component analysis (PCA) showed that all five chronologies loaded positively on the first principal component (PC1). PC1 explained 67.5% of the total variance among all residual chronologies (Fig. S1, Table S2). Such a high amount of variance explained by PC1 indicates the strong common growth signal under the common environmental forcing along elevational gradients in both sites. However, temporal divergence was observed in ring-width index curves during the 1990s, when the lower elevation (3900 m) site showed higher growth than the other two sites in the BSM (Fig. 4c). Reanalysis of ring-width index series with subsamples of equal sample depth along elevation gradients for the period 1901–2015 also revealed the same chronology signals (Fig. S2), and thus confirmed the abnormal growth during 1990s at lower elevation in the BSM. Similarly, variations in the ring-width index series were observed around the 1830s and 1870s at upper and lower elevations in the SSM, which could be related to abrupt declining of sample depth before 1900s. The running expressed population signal (EPS) curves passed an arbitrary threshold value of 0.85 up to 1915 for upper and middle elevation and up to 1840 at lower elevation in the BSM. Meanwhile, the EPS curves in the SSM were dropped below the 0.85 threshold before 1860s and 1875s at upper and lower elevations, respectively (Fig. 4).

The average annual radial growth rate (AGR) and growth variability from the mean (SD) were found to decrease along the elevation gradient in both the BSM and SSM sites (Table 2). The mean sensitivity (MS) in both sites was decreasing with elevation. Meanwhile, inter-series correlations (Rbar), signal-to-noise ratio (SNR), and EPS increased along with elevation in both study sites (Table 2). Rbar was high in both sites and ranged from 0.435 to 0.514 in the BSM and from 0.398 to 0.464 in the SSM. The SNR values ranged from 31.18 to 87.11 in the BSM and from 7.81 to 9.92 in the SSM, indicating strong common climatic signals retained in the chronologies (Table 2), as it is also indicated by EPS values passing the 0.85 threshold. The high values of Rbar, SNR and EPS in both sites confirm the reliable quality of all tree-ring chronologies for further analyses of climate-growth responses. Their elevational trends indicate a stronger climatic forcing of tree growth patterns at higher elevations.

Tree growth of Yunnan fir showed a positive relationship with summer temperatures, of which July minimum and mean temperatures were most important and consistent along elevational gradients in both study sites (Figs. 5 and 6). The temporal climate-growth response revealed much stronger correlations with June minimum and mean temperatures during late sub-period compared to early sub-period and the entire period of climate data. Similar relationships were observed for chronologies with subsamples of equal sample depth along elevation gradients (Figs. S3 and S4), though the strength of correlations was different. Correlations with July mean and minimum temperature were higher at upper and middle elevations than at lower elevation band (Figs. 5–7, S3 and S4). In contrast, summer precipitation, mean relative humidity (RH) and SPEI showed negative relationships with tree growth in both study sites (Figs. 7, S3 and S4). Though the relationships were much stronger in early sub-periods and the entire period of climate data, a decline in the strength of negative correlations occurred with June moisture (precipitation, RH and SPEI) in the later sub-period (Figs. 5 and 6) at all elevations in both BSM and SSM. Similarly, tree growth showed negative relationships with spring temperatures in both BSM and SSM. The negative relationship was much stronger during early sub-period but the strength of relationship declined in the late sub-period. For the entire period, negative correlation with May minimum temperature was most important for all elevation bands in both sites (Figs. 5 and 6). Meanwhile, February moisture availability (precipitation, RH and SPEI) showed positive relationships with tree growth. In the meantime, tree growth showed positive correlations with winter temperatures, though the correlation was not strong for the entire period of data. The positive relationship during the early sub-period was much stronger in early winter months, while the strength of correlation decreased during late sub-period and the relationship shifted to late winter months. However, positive relationships with previous November temperature were consistent for the entire period in all elevation bands at both sites (Figs. 5 and 6).

4. Discussion

Our results revealed decreasing average growth rates of high-elevation Yunnan fir trees with increasing elevation in the Hengduan Mountains. Decreasing tree growth with elevation was also observed on the southern Tibetan Plateau (Liang et al., 2010; Lyu et al., 2016, 2017), and in the Tianshan Mountains (Huo et al., 2017). The high

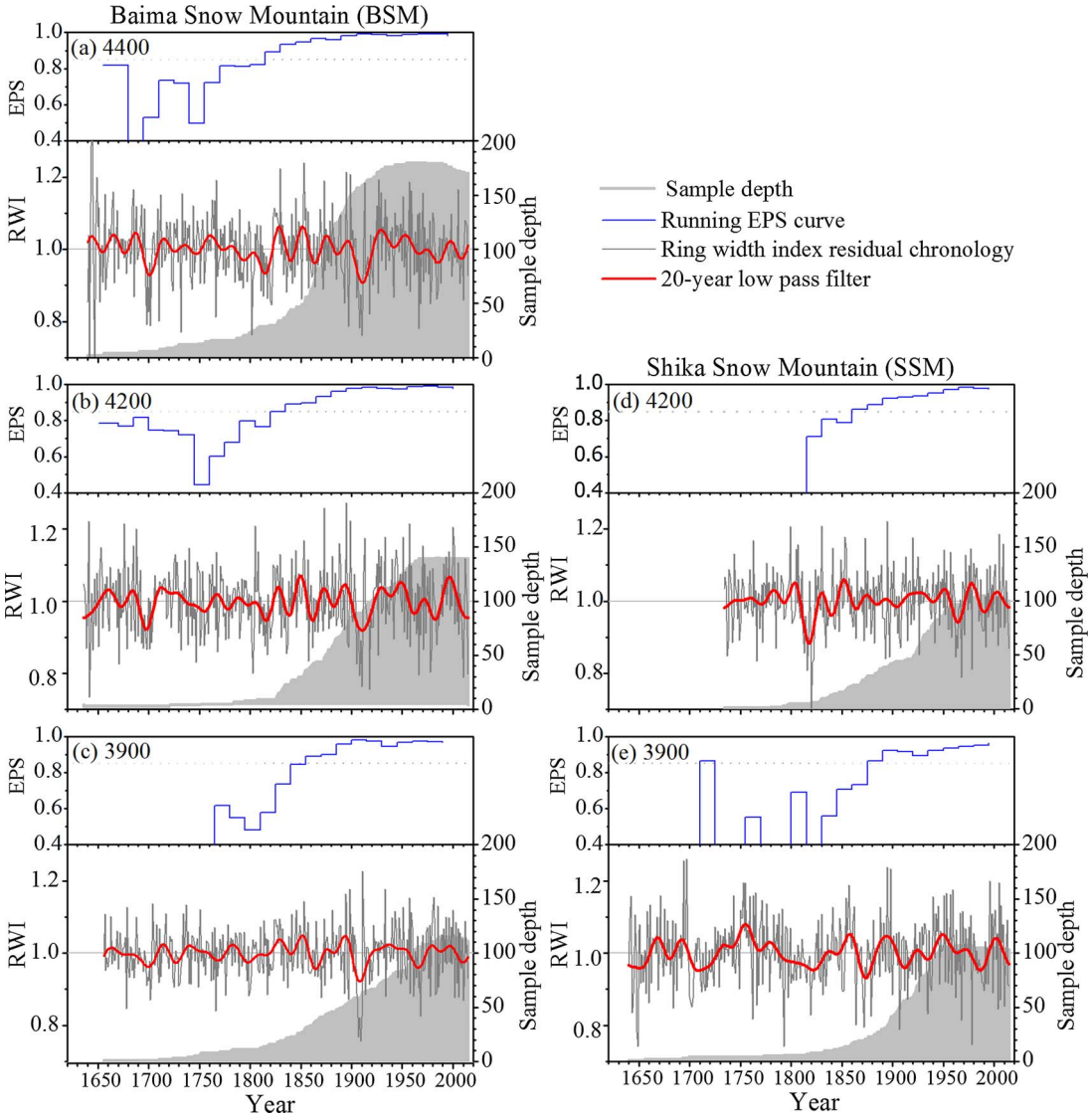

Fig. 4. Tree-ring width residual chronologies of Yunnan fir along elevation gradients in the BSM (left panel) and the SSM (right panel) with annual variation in ring-width index (black line), 20-year low-pass filter (red line), sample depth (grey shading), and EPS curve (blue line). (For interpretation of the references to color in this figure legend, the reader is referred to the web version of this article.)

Table 3
Pearson correlation coefficients between tree-ring width residual chronologies of BSM and SSM sites along elevation gradients for the common period 1850–2015 (N = 166, average correlation across sites, r = 0.582***). Significance level: *** $p \leq 0.001$.

	B2_4400	B2_4200	B2_3900	S2_4200	S2_3900
B2_4400	1.000	0.827***	0.570***	0.588***	0.429***
B2_4200		1.000	0.640***	0.589***	0.505***
B2_3900			1.000	0.518***	0.521***
S2_4200				1.000	0.633***
S2_3900					1.000

growth synchronicity of Yunnan fir forests indicates a strong common environmental forcing along the studied elevation gradient. Nevertheless, tree radial growth rates and growth response to climate provide evidence for elevational trends. As elevation increases, climatic harshness increases (Liang et al., 2014) and tree growth becomes more sensitive to the harsher environmental conditions (Körner, 2012). The low temperatures at higher elevation may physiologically constrain carbon assimilation (Körner, 2015) and thus inhibit the xylem tissue differentiation and structural investment (Rossi et al., 2008; Li et al., 2017b) in the cold environment of the Hengduan Mountains. A positive influence of increasing growing season length on xylem production of conifers in the Tibetan plateau and other temperature-limited sites has already been detected (Rossi et al., 2008; Li et al., 2017b; Yang et al., 2017).

The negative correlations between radial growth and spring temperatures indicate that moisture conditions during the early growing season are a limiting factor for tree growth in high-elevation forests of Yunnan fir. Negative relationships of tree growth with spring and early growing season temperatures were reported by several studies in high-elevation forests of the Hengduan Mountains (Fan et al., 2008b, 2009a,b; Bi et al., 2015), in the south-eastern Tibetan Plateau (Bräuning and Grießinger, 2006; Li et al., 2017a), in the central (Dawadi et al., 2013; Liang et al., 2014; Kharal et al., 2017; Panthi et al., 2017), and in the western Himalayas (Sohar et al., 2017). High spring temperatures enhance evapotranspiration and thus induce drought stress which delays the onset of xylogenesis and xylem cell production and finally controls tree growth of high elevation forests (Fan et al., 2008a,b; Liang et al., 2014; Ren et al., 2015; Li et al., 2017a). In contrast, the positive relationship of tree radial growth with winter temperatures in the central HM is supported by previous studies (e.g. Fan et al., 2009a).

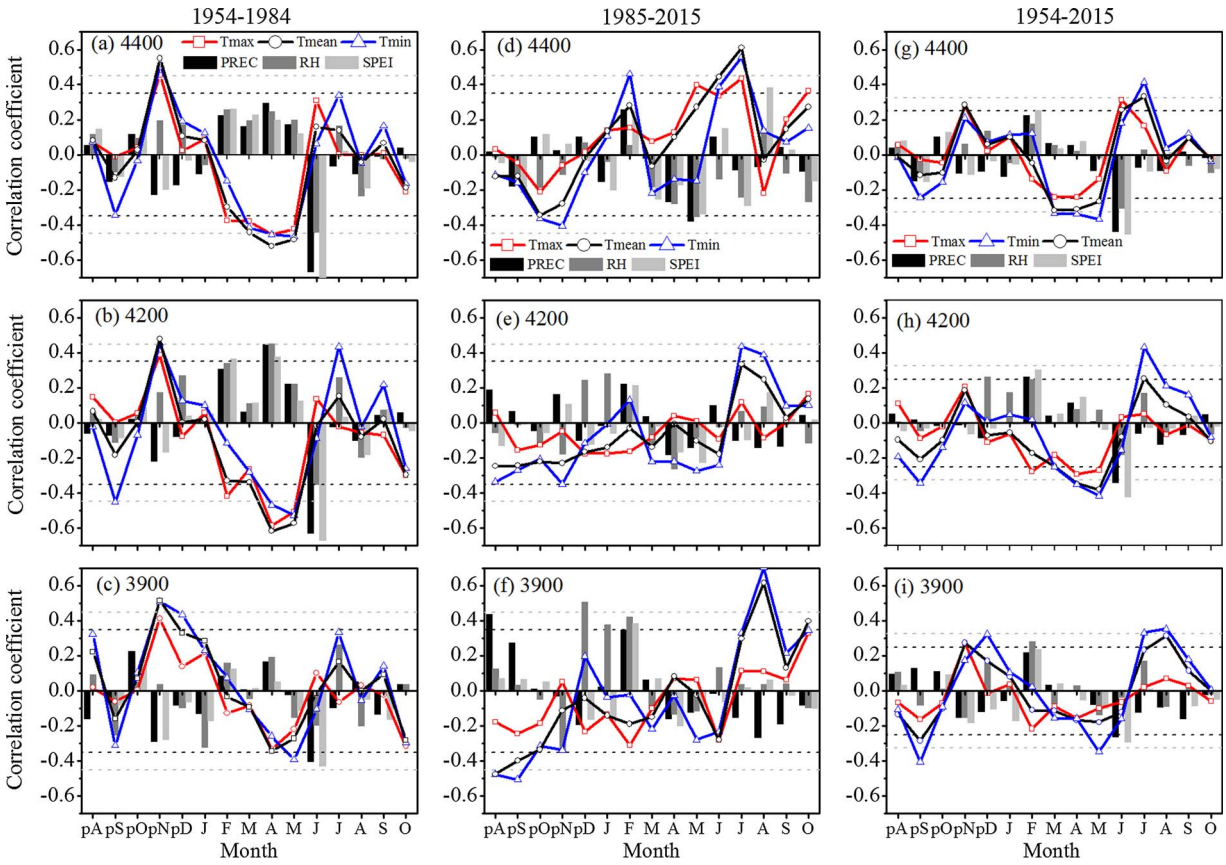

Fig. 5. Correlation coefficients of residual chronologies in the BSM with first-differences of monthly climate data of Deqin from previous August to current October over the periods 1954–1984 (left panel), 1985–2015 (middle panel) and 1954–2015 (right panel). Temperatures (line-circles) and precipitation (black bars), relative humidity (grey bars) and SPEI (light grey bars). Horizontal dashed black and grey lines indicate the 95% and 99% confidence levels, respectively.

Though the winter is too cold and cambial activity is still inactive, warmer winter temperature may protect the needles from frost damage and maintain them photosynthetically active for the following year. Furthermore, tree growth responds positively to February precipitation and moisture availability (RH and SPEI) in the semi-arid winter/early spring conditions of our study area. February precipitation is probably related to refilling soil water reservoirs before spring, which then may be available during the onset of xylogenesis. The stronger positive relationship with February precipitation for radial tree growth in the SSM sites can be explained by the fact that the amount of spring

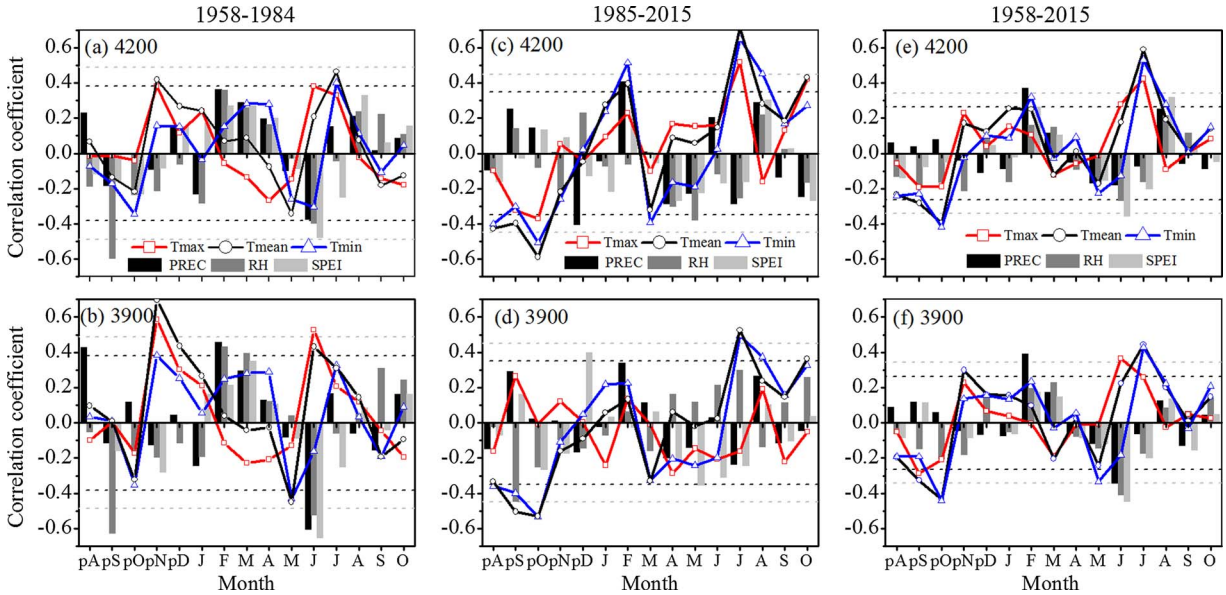

Fig. 6. Correlation coefficients of residual chronologies in the SSM with first-differences of monthly climate data of Shangri-la from previous August to current October over the periods 1958–1984 (left panel), 1985–2015 (middle panel) and 1958–2015 (right panel). Temperatures (line-circles) and precipitation (black bars), relative humidity (grey bars) and SPEI (light grey bars). Horizontal dashed black and grey lines indicate the 95% and 99% confidence levels, respectively.

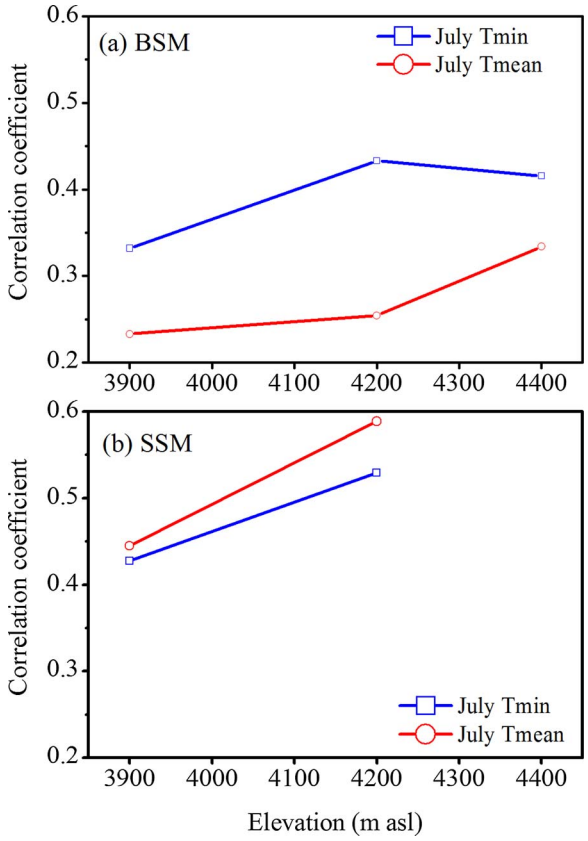

Fig. 7. Elevational trends in correlation coefficients of Yunnan fir with July minimum (blue line-circle) and mean (red line-circle) temperatures: (a) BSM during 1954–2015, and (b) SSM during 1958–2015. (For interpretation of the references to color in this figure legend, the reader is referred to the web version of this article.)

precipitation in SSM is considerably lower than in the BSM (Fig. 2a, b). The positive relationship with early spring precipitation/moisture availability is supported by several studies in other high mountain regions of Asia (Fan et al., 2009a; Dawadi et al., 2013; Liang et al., 2014; Panthi et al., 2017).

Summer temperature (mainly July minimum and/or mean temperature) has been found to be the most important factor determining radial growth rates of *A. georgei* in the HM. Tree growth in high-elevation ecosystems with very humid summer conditions is usually favored by higher summer temperatures (Fan et al., 2009a,b; Liang et al., 2009, 2010), and this relationship becomes stronger at higher elevations. Several studies provided evidence that increased minimum temperatures play an important role to enhance xylem tissue formation in cold environments of high-elevation forests (Bräuning and Mantwill, 2004; Liang et al., 2009, 2010; Li et al., 2013). Liang et al. (2010) and Li et al. (2013) demonstrated that in high-elevation fir forests on the southeastern Tibetan Plateau, minimum temperature rather than maximum temperature is a dominant regulator of fir growth. Elevated summer temperatures may induce an earlier start of cambial activity (Begum et al., 2013), as well as higher rates of cambial growth and xylem cell production (Rossi et al., 2014). The increase in strength of the correlation between ring width and the increasing July minimum and mean temperatures (Fig. 3) at all elevations in both BSM and SSM (Figs. 5 and 6) supports the hypothesis that tree radial growth benefits from elevated growing season temperatures. The positive relationship of tree radial growth with summer temperatures is supported by studies conducted on the southern Tibetan Plateau (Bräuning and Mantwill, 2004). Moreover, higher correlations between radial growth and summer temperatures at higher elevations were also found on the southern Tibetan plateau by Liang et al. (2009) and Lyu et al. (2017).

The positive relationship to temperature conditions is supported by negative correlations of radial growth with summer (mainly that of June) precipitation and moisture availability. June is the transition month for abrupt decreasing total sunshine duration and increasing the precipitation and relative humidity (Fig. 2). After the summer monsoon onset in late May or early June, the HM receives sufficient summer precipitation for tree growth from June to August or early September (Fig. 2a, b). The summer monsoon increases low level cloud cover and the frequency of foggy conditions, when local convective cloud cover increases during the daytime at high and middle elevations. Clouds and fog reduce solar radiation input and photosynthetic active radiation by decreasing the total sunshine duration (Fig. 2c, d), which may have adverse effects on tree growth compared to lower elevation belts located below the cloud condensation level.

5. Conclusions

We reveal an elevational trend on tree growth and growth responses to climatic variability of high-elevation Yunnan fir (*Abies georgei*) forests along elevation gradients from two sites in the central Hengduan Mountains. Correlation analyses revealed that tree growth was limited by summer temperature and that the strength and magnitude of growth-climate relationships was enhanced with increasing elevation. The stronger positive relationships with July temperatures in the later sub-period compared to the early sub-period reveal that tree radial growth benefits from increased summer temperatures. Currently, summer precipitation in our humid study region is still sufficient to satisfy the moisture demand of high-elevation trees under warmer growing-season temperatures. However, the increasing trend of annual mean temperatures accompanied by a decreasing trend of annual mean RH may lead to increasing evapotranspiration and moisture stress in the HM.

Conflicts of interest

The authors declare no competing financial and any other potential conflict of interests.

Acknowledgements

This work was funded by the National Natural Science Foundation of China (NSFC, 31770533, 31370496, U1502231) and National Key Research Development Program of China (2016YFC0502105). Meteorological data for Deqin and Shangri-la stations were obtained from National Meteorological Information Center (NMIC), China. Special thanks to Prof. Richard T. Corlett, Dr. Pei-Li Fu, and two anonymous reviewers for their valuable comments and suggestions on the manuscript. Mr. Hong Ma and Mr. Mei-Yi Tan are thankful for their assistances during the field work.

Appendix A. Supplementary data

Supplementary data associated with this article can be found, in the online version, at http://dx.doi.org/10.1016/j.dendro.2017.11.001.

References

Begum, S., Nakaba, S., Yamagishi, Y., Oribe, Y., Funada, R., 2013. Regulation of cambial activity in relation to environmental conditions: understanding the role of temperature in wood formation of trees. Physiol. Plant. 147 (1), 46–54.

Bi, Y., Xu, J., Gebrekirstos, A., Guo, L., Zhao, M., Liang, E., Yang, X., 2015. Assessing drought variability since 1650 AD from tree-rings on the Jade Dragon Snow Mountain, southwest China. Int. J. Climatol. 35, 4057–4065.

Bräuning, A., Grießinger, J., 2006. Late Holocene variations in monsoon intensity in the Tibetan–Himalayan region-evidence from tree rings. J. Geol. Soc. India 68 (3), 485–494.

Bräuning, A., Mantwill, B., 2004. Summer temperature and summer monsoon history on the Tibetan Plateau during the last 400 years recorded by tree rings. Geophys. Res.

Lett. 31, L24205.
Bräuning, A., 2001. Combined view of various tree ring parameters from different habitats in Tibet for the reconstruction of seasonal aspects of Asian Monsoon variability. Palaeobot. 50, 1–12.
Briffa, K.R., Jones, P.D., 1990. Basic chronology statistics and assessment. In: Cook, E.R., Kairiukstis, L.A. (Eds.), Methods of Dendrochronology: Application in Environmental Science. Kluwer Academic Press, Netherlands.
Böhner, J., 2006. General climatic controls and topoclimatic variations in Central and High Asia. Boreas 35, 279–295.
Cook, E.R., Briffa, K.R., 1990. A comparison of some tree-ring standardization methods. In: Cook, E.R., Kairiukstis, L.A. (Eds.), Methods of Dendrochronology: Application in Environmental Science. Kluwer Academic Press, Netherlands.
Cook, E.R., Peters, K., 1997. Calculating unbiased tree-ring indices for the study of climatic and environmental change. Holocene 7, 361–370.
Cook, E.R., 1985. A Time-Series Analysis Approach to Tree-Ring Standardization. The University of Arizona, Tucson Ph.D. dissertation.
Dawadi, B., Liang, E., Tian, L., Devkota, L.P., Yao, T.S., 2013. Pre-monsoon precipitation signal in tree rings of timberline *Betula utilis* in the central Himalayas. Quat. Int. 283, 72–77.
Fan, Z.-X., Thomas, A., 2013. Spatiotemporal variability of reference evapotranspiration and its contributing climatic factors in Yunnan Province, SW China, 1961-2004. Clim. Change 116, 309–325.
Fan, Z.-X., Bräuning, A., Cao, K.-F., 2008a. Annual temperature reconstruction in the central Hengduan Mountains, China, as deduced from tree rings. Dendrochronologia 26, 97–107.
Fan, Z.-X., Bräuning, A., Cao, K.-F., 2008b. Tree-ring based drought reconstruction in the central Hengduan Mountains region (China) since AD 1655. Int. J. Climatol. 28 (14), 1879–1887.
Fan, Z.-X., Bräuning, A., Cao, K.-F., Zhu, S.-D., 2009a. Growth–climate responses of high-elevation conifers in the central Hengduan Mountains, southwestern China. For. Ecol. Manag. 258, 306–313.
Fan, Z.-X., Bräuning, A., Yang, B., Cao, K.-F., 2009b. Tree ring density-based summer temperature reconstruction for the central Hengduan Mountains in southern China. Glob. Planet. Change 65, 1–11.
Fan, Z.-X., Bräuning, A., Thomas, A., Li, J.-B., Cao, K.-F., 2011. Spatial and temporal temperature trends on the Yunnan Plateau (Southwest China) during 1961–2004. Int. J. Climatol. 31, 2078–2090.
Frenzel, B., Bräuning, A., Adamczyk, S., 2003. On the problem of possible late-glacial forest refuge-area with the deep valleys of Eastern Tibet. Erdkunde 57, 182–198.
Fritts, H.C., 1976. Tree Rings and Climate. Elsevier, New York.
Huo, Y., Gou, X., Liu, W., Li, J., Zhang, F., Fang, K., 2017. Climate–growth relationships of Schrenk spruce (*Picea schrenkiana*) along an altitudinal gradient in the western Tianshan Mountains, northwest China. Trees 31 (2), 429–439. http://dx.doi.org/10.1007/s00468-017-1524-8.
Kharal, D.K., Thapa, U.K., George, S.S., Meilby, H., Rayamajhi, S., Bhuju, D.R., 2017. Tree-climate relations along an elevational transect in Manang Valley, central Nepal. Dendrochronologia 41, 57–64. http://dx.doi.org/10.1016/j.dendro.2016.04.004.
Kier, G., Mutke, J., Dinerstein, E., Ricketts, T.H., Küper, W., Kreft, H., Barthlott, W., 2005. Global patterns of plant diversity and floristic knowledge. J. Biogeogr. 32, 1107–1116.
Körner, C., 2012. Alpine Treelines: Functional Ecology of the Global High Elevation Tree Limits. Springer.
Körner, C., 2015. Paradigm shift in plant growth control. Curr. Opin. Plant Biol. 25, 107–114.
Li, Z.S., Li, G.H., Fu, B.J., Hu, C.J., Luo, S.Z., Liu, X.L., He, F., 2012a. Anomalous temperature-growth response of *Abies faxoniana* to sustained freezing stress along elevational gradients in China's Western Sichuan Province. Trees 26, 1373–1388.
Li, Z.-S., Zhang, Q.-B., Ma, K., 2012b. Tree-ring reconstruction of summer temperature for A.D. 1475–2003 in the central Hengduan Mountains, Northwestern Yunnan, China. Clim. Change 110, 455–467. http://dx.doi.org/10.1007/s10584-011-0111-z.
Li, X., Liang, E., Gričar, J., Prislan, P., Rossi, S., Čufar, K., 2013. Age dependence of xylogenesis and its climatic sensitivity in Smith fir on the south-eastern Tibetan Plateau. Tree Physiol. 33 (1), 48–56.
Li, J., Shi, J., Zhang, D.D., Yang, B., Fang, K., Yue, P.H., 2017a. Moisture increase in response to high-altitude warming evidenced by tree-rings on the southeastern Tibetan Plateau. Clim. Dyn. 48, 649–660. http://dx.doi.org/10.1007/s00382-016-3101-z.
Li, X., Liang, E., Gričar, J., Rossi, R., Čufar, K., Ellison, A.M., 2017b. Critical minimum temperature limits xylogenesis and maintains treelines on the southeastern Tibetan Plateau. Sci. Bull. 62, 804–812.
Liang, E., Shao, X., Xu, Y., 2009. Tree-ring evidence of recent abnormal warming on the southeast Tibetan Plateau. Theor. Appl. Climatol. 98, 9–18.
Liang, E., Wang, Y., Xu, Y., Liu, B., Xuemei, S., 2010. Growth variation in *Abies georgei* var. *smithii* along altitudinal gradients in the Sygera Mountains southeastern Tibetan Plateau. Trees 24, 363–373.
Liang, E., Dawadi, B., Pederson, N., Eckstein, D., 2014. Is the growth of birch at the upper timberline in the Himalayas limited by moisture or by temperature? Ecology 95, 2453–2465.
Liang, E., Leuschner, C., Dulamsuren, C., Wagner, B., Hauck, M., 2016. Global warming-related tree growth decline and mortality on the north-eastern Tibetan plateau. Clim. Change 134, 163–176. http://dx.doi.org/10.1007/s10584-015-1531-y.
Liu, J., Qin, C., Kang, S., 2013. Growth response of *Sabina tibetica* to climate factors along an elevation gradient in south Tibet. Dendrochronologia 31, 255–265. http://dx.doi.org/10.1016/j.dendro.2012.12.001.
Lyu, L., Deng, X., Zhang, Q.-B., 2016. Elevation pattern in growth coherency on the southeastern Tibetan Plateau. PLoS One 11 (9), e0163201. http://dx.doi.org/10.1371/journal.pone.0163201.
Lyu, L., Suvanto, S., Nöjd, P., Henttonen, H.M., Mäkinen, H., Zhang, Q.-B., 2017. Tree growth and its climate signal along latitudinal and altitudinal gradients: comparison of tree rings between Finland and Tibetan Plateau. Biogeosci. Discuss. 14, 3083–3095. http://dx.doi.org/10.5194/bg-2016-559.
Mountain Research Initiative EDW Working Group, 2015. Elevation dependent warming in mountain regions of the world. Nat. Clim. Change 5, 424–430.
Myers, N., Mittermeier, R.A., Mittermeier, C.G., da Fonseca, G.A.B., Kent, K., 2000. Biodiversity hotspots for conservation priorities. Nature 403, 853–855.
Osborn, T.J., Briffa, K.R., Jones, P.D., 1997. Adjusting variance for sample-size in tree-ring chronologies and other regional mean timeseries. Dendrochronologia 15, 89–99.
Panthi, S., Bräuning, A., Zhou, Z.-K., Fan, Z.-X., 2017. Tree rings reveal recent intensified spring drought in the central Himalaya, Nepal. Glob. Planet. Change 157, 26–34. http://dx.doi.org/10.1016/j.gloplacha.2017.08.012.
Ren, P., Rossi, S., Gricar, J., Liang, E., Cufar, K., 2015. Is precipitation a trigger for the onset of xylogenesis in *Juniperus przewalskii* on the north-eastern Tibetan Plateau? Ann. Bot. 115, 629–639.
Rinn, F., 2003. TSAP-Win User Reference Manual. Rinntech, Heidelberg.
Rossi, S., Deslauriers, A., Gričar, J., Seo, W., Rathgeber, C.B.K., Anfodillo, T., Morin, H., Levanic, T., Oven, P., Jalkanen, R., 2008. Critical temperatures for xylogenesis in conifers of cold climates. Glob. Ecol. Biogeogr. 17, 696–707.
Rossi, S., Girard, M.J., Morin, H., 2014. Lengthening of the duration of xylogenesis engenders disproportionate increases in xylem production. Glob. Change Biol. 20 (7), 2261–2271.
Schweingruber, F.H., 1996. Tree Rings and Environment-Dendrochronology. Haupt, Bern.
Sohar, K., Altman, J., Lehěcková, E., Doležal, J., 2017. Growth–climate relationships of Himalayan conifers along elevational and latitudinal gradients. Int. J. Climatol. 37 (5), 2593–2605. http://dx.doi.org/10.1002/joc.4867.
Stokes, M.A., Smiley, T.L., 1996. An Introduction to Tree-Ring Dating. Arizona Uni. Press, Chicago.
Vicente-Serrano, S.M., Beguería, S., López-Moreno, J.I., 2010. A multiscalar drought index sensitive to global warming: the standardized precipitation evapotranspiration index. J. Clim. 23 (7), 1696–1718.
Wang, W., Jia, M., Wang, G., Zhu, W., McDowell, N.G., 2017. Rapid warming forces contrasting growth trends of subalpine fir (*Abies fabri*) at higher- and lower-elevations in the eastern Tibetan Plateau. For. Ecol. Manag. 402, 135–144.
Wigley, T.M.L., Briffa, K.R., Jones, P.D., 1984. On the average value of correlated time series, with applications in dendroclimatology and hydrometeorology. J. Clim. App. Meteorol. 23, 201–213.
Wu, Z.Y., Raven, P.H. (Eds.), 1999. Flora of China, Vol. 4 (Cycadaceae-Fagaceae). Science Press and Missouri Botanical Garden Press, Beijing and St Louis, pp. 44–52.
Xia, X., 2010. Spatiotemporal changes in sunshine duration and cloud amount as well as their relationship in China during 1954-2005. J. Geophy. Res. 115, D00K06. http://dx.doi.org/10.1029/2009JD012879.
Xing, Y.-W., Ree, R.H., 2017. Uplift-driven diversification in the Hengduan Mountains, a temperate biodiversity hotspot. Proc. Natl. Acad. Sci. U. S. A. E3444–E3451. http://dx.doi.org/10.1073/pnas.1616063114.
Yang, B., He, M., Shishov, V., Tychkov, I., Vaganove, E., Rossi, S., Ljungqvist, F.C., Bräuning, A., Grießinger, J., 2017. New perspective on spring vegetation phenology and global climate change based on Tibetan Plateau tree-ring data. Proc. Natl. Acad. Sci. U. S. A. 114 (27), 6966–6971. http://dx.doi.org/10.1073/pnas.1616608114.
Zhang, Q.-Y., Luo, P., Zhang, Y.-C., Shi, F.-S., Yi, S.-L., Wu, N., 2008. Ecological characteristics of *Abies georgei* population at timberline on the north-facing slope of Baima Snow Mountain, Southwest China. Acta Ecol. Sin. 28 (1), 129–135.